EARTHQUAKE ENGINEERING AND STRUCTURAL DYNAMICS
Earthquake Engng. Struct. Dyn. **28**, 1019–1039 (1999)

EXPERIMENTAL STUDY OF IDENTIFICATION AND CONTROL OF STRUCTURES USING NEURAL NETWORK PART 2: CONTROL

KHALDOON BANI-HANI[†], JAMSHID GHABOUSSI[‡,*] AND STEPHEN P. SCHNEIDER[¶]
Department of Civil Engineering, University of Illinois at Urbana Champaign, Urbana, IL 61801, USA

SUMMARY

Experimental verifications of a recently developed active structural control method using neural networks are presented in this paper. The experiments were performed on the earthquake simulator at the University of Illinois at Urbana—Champaign. The test specimen was a 1/4 scale model of a three-storey building. The control system consisted of a tendon/pulley system controlled by a single hydraulic actuator at the base. The control mechanism was implemented through four active pre-tensioned tendons connected to the hydraulic actuator at the first floor. The structure modelling and system identification has been presented in a companion paper. (*Earthquake Engng. Struct. Dyn.* **28**, 995–1018 (1999)). This paper presents the controller design and implementation. Three controllers were developed and designed: two neurocontrollers, one with a single sensor feedback and the other with three sensor feedback, and one optimal controller with acceleration feedback. The experimental design of the neurocontrollers is accomplished in three steps: system identification, multiple emulator neural networks training and finally the neurocontrollers training with the aid of multiple emulator neural networks. The effectiveness of both neurocontrollers are demonstrated from experimental results. The robustness and the relative stability are presented and discussed. The experimental results of the optimal controller performance is presented and assessed. Comparison between the optimal controller and neurocontrollers is presented and discussed. Copyright © 1999 John Wiley & Sons, Ltd.

KEY WORDS: structures; dynamics; control; neural networks; earthquake engineering

INTRODUCTION

The attraction of developing intelligent, robust and adaptive systems has fascinated many researchers in the civil engineering applications. In early 1970s Yao[1] introduced the framework of a new generation of civil structure using active control system. Since this time, researchers have conducted studies to develop new methods in active and passive structural control. Some of

* Correspondence to: Jamshid Ghaboussi, Department of Civil Engineering, University of Illinois at Urbana Champaign, 3118 Newmark Civil Engineering Laboratory, MC-250, 205 North Mathews Ave., Urbana, Illinois 61801-2397, USA.
[†] Assistant Professor, Jordan University of Science and Technology, Jordan.
[‡] Professor of Civil Engineering
[¶] Associate Professor of Civil Engineering

CCC 0098–8847/99/091019–21$17·50

Received 17 September 1998
Accepted 25 March 1999

these have been proven to be suitable and robust for civil structures.[2,3] Unfortunately, few of these studies have been implemented experimentally.[4–9] This paper continues the presentation of a comprehensive experimental study[10] that has been conducted in an effort to verify a recently proposed neural network based approach in structural control. This study comprises the first experiments in neural network based structural control. The first part of this study, represents the system identification and the emulator developments, has been presented in a previous companion paper.[10] In this paper, the full description of the controllers design and their implementation are presented and discussed.

In the last few years, many researchers have been engaged in the use of neural networks almost in every field of engineering with the intent of finding better solutions to conventional methods. In the field of control, neural networks have been found to be well suited for complex linear and non-linear control problems. This paper presents evidence of the potential powerful capabilities of neural networks in structural control. The experiments have been conducted on the shaking table at the University of Illinois at Urbana—Champaign. The method of structural control using neural networks has been proposed and developed over the past few years by Ghaboussi and his co-workers. A neurocontrol method based on the inverse transfer function was developed by Nikzad and Ghaboussi[11] and applied in an experimental study of the actuator dynamics and delay compensation.[12] A neurocontrol method which utilized an emulator neural network in its training, was developed and applied in linear and non-linear structural control problems.[13–20] A similar method has been proposed by Chen *et al.*[21] In the neural network based method a neurocontroller *learns* how to control the structure under dynamic excitation, unlike the mathematical control algorithms which explicitly formulate the control task. The neurocontroller acquires the knowledge of the control strategies through training process and stores the knowledge in inter-neurons connection weights.

The experiments reported in this study were organized in three successive phases. The first and second phases were presented in the first companion paper.[10] The third phase consisted of the development and design of the controllers. Two neurocontrollers with different architectures, feedbacks and sampling rates were developed and trained with the aid of the prediction capabilities of multiple neuro-emulators (EU3AI, EU3AII, EU3AIII, EUAI, EUAII and EUAIII).[10] Also, one optimal controller was designed and tested for comparison. The first neurocontroller, referred to as U3A, uses the three absolute accelerations of the three floors as feedback to control future vibrations of the structure. The second neurocontroller, referred to as UA, uses the *third floor* absolute acceleration as the single feedback. The robust-ness and stability of both neurocontrollers were demonstrated experimentally. The optimal controller uses the three absolute accelerations of the three floors as feedback, as shown in Figure 1. The experimental performance of the optimal controller is demonstrated. A comparison between the experimental results of the neurocontrollers and the optimal controller is presented in this paper.

The experiments were conducted on the earthquake simulator at the University of Illinois at Urbana—Champaign (Figure 2). The test specimen is a 1/4 scale model of a three-storey steel frame fully instrumented to provide a full description of its motion. The control system consists of four active tendons connected to the control actuator and the first floor. The controllers have been implemented digitally through a Power PC computer. The neurocontroller simulators were written using LabVIEW[22] instrumentation software, which acquire the needed feedback sensor reading(s), simulate(s) the neural network computation and issue(s) the control signal to an INSTRON Plus 8500 digital unit through the NB-MIO-16X board. Moreover, the optimal controller was also performed using the LabVIEW[22] instrumentation software. The full

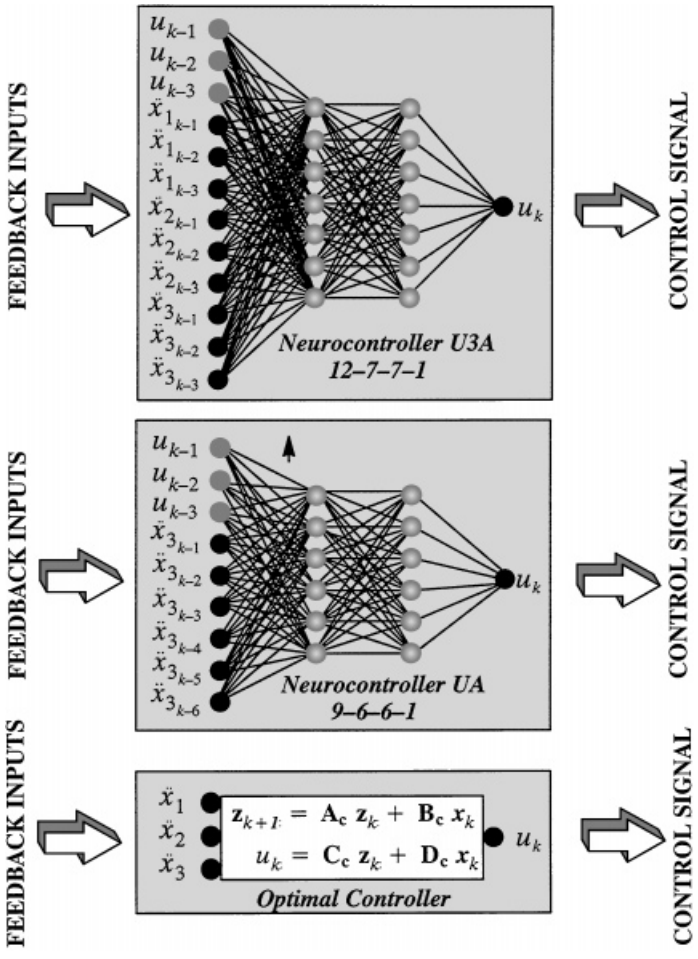

Figure 1. The architecture of both neurocontrollers (U3A and UA) as well as the optimal controller

description of the test set-up and the test specimen, the control system, the hardware/software implementation of the controllers and the system modelling was discussed thoroughly in the previous companion paper by Bani-Hani *et al.*[10]

OUTLINE OF THE NEURO-CONTROL STRATEGY

The concept of neuro-control is meant to describe the use of a well-specified neural network to issue actual control signal to a designated control system. The neurocontroller replaces the feedback control algorithm in a conventional control method. The neurocontroller receives the feedback information at its input layer and issues an appropriate signal to the control system from its output layer. Typical neurocontrollers are shown in Figure 1. In the software

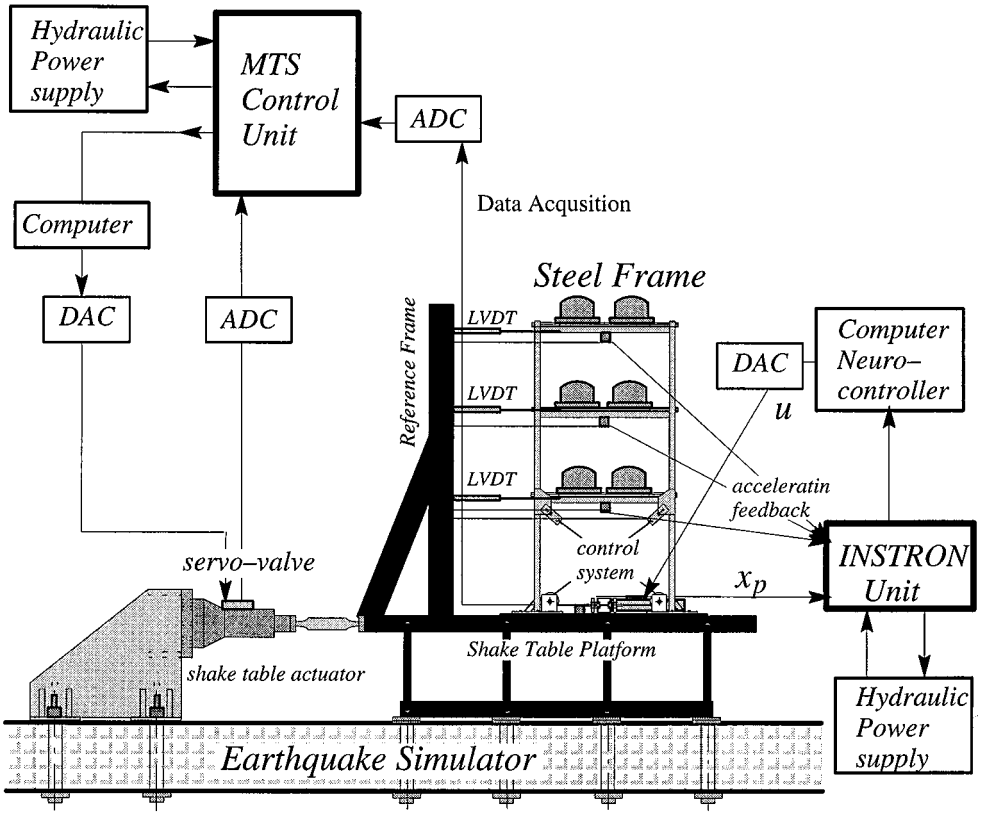

Figure 2. The experimental set-up and schematic implementation of the control experiments

implementation of the neuro-controller, the sensor data is received at discrete time intervals, referred to as the sampling periods, T_s. The output of the neurocontroller is also sent to the control system at the same discrete sampling period.

In a digital control setting, the neurocontroller learns a relationship that can be described as follows: Consider a controlled structure subjected to a load vector $\boldsymbol{p}$ and actuator signal vector $\boldsymbol{u}$ and let $\boldsymbol{y}$ and $\boldsymbol{z}$ be the vector of sensor readings and output vector, respectively. The relationship that the neurocontroller learns must exist, otherwise the training process will not be successful. The uniqueness requirements for neural networks are far more relaxed than for mathematical functions. For the neural network training to be successful, the relationship must exist but need not be strictly unique. Moreover, even if the underlying function uniquely exists, the neural network architecture is not unique; more than one neural network can learn the same relationship to within a given degree of accuracy. We assume that the following function, which has to be learned by the neural networks, defining the future value of the actuator signal, subject to some constraint, does exist.

$$u_{k+1} = f_{nc}(y_k, y_{k-1}, \ldots, y_{k-\ell}, u_k, u_{k-1}, \ldots, u_{k-m}, p_k, p_{k-1}, \ldots, p_{k-n}) \quad (1)$$

$$\text{subject to} \qquad \bar{f}_{nc}(z_{k+1}, z_{k+2}, \ldots, z_{k+p}) < \varepsilon$$

Note that the arguments of the function include a portion of the past history of the sensor readings, actuator signal and loading. The constraint equation is a function of the future values of the output vector. The main parameters of this function are the extent of the past and future digital values of the arguments ℓ, m, n and p. Such a relationship would always exist for sufficiently large values of ℓ, m, n and sufficiently small value of p. These parameters are in general related to the order and the degree of non-linearity of underlying process represented by the function. Currently, there are no rigorous methods of determining these parameters, however, a trial and error process usually produce an acceptable result. It is important to note that the function in equation (1), which must be learned by the neurocontroller also includes the effects of actuator dynamic, actuator saturation, time delays and the sampling period. It is, therefore, a highly non-linear function, even if the structural behavior is strictly linear.

The neuro-control training method, first proposed by Ghaboussi *et al.*[15,17] requires an emulator neural network. In this paper, we have developed a variation of the method which employs three emulator neural networks[10] to make more accurate predictions of the future values of the structural response. These emulator neural networks were used to train the neurocontrollers.

Neuro-control methodology

Neural network based methods in structural control, have been proposed and tested in many previous publications.[12,13,15–20] Through these few years, a continuous effort in improving and verifying the methods have been introduced and tested. The control scheme used in this study has been mentioned in recent publications.[17,18] However, this method has been improved to achieve better, higher control performance by enhancing the prediction capability using multiple emulator neural networks.

Training the neurocontroller has been in parallel-series fashion with the use of multiple emulator neural networks. The training procedure of the neurocontroller is shown schematically in Figure 3. Mathematical implementation of the underlying methodology, can be approached in different ways. In this study, a simple and numerically stable approach has been used. In training the neurocontroller, the objective is to find the appropriate control signal that achieves the control criterion. However, this knowledge is not available to the designer a priori. Therefore, with the aid of independent neural networks, the control signal is predicted and estimated. The neuro-control method is based on an iterative search for the control signal u that achieves the control criterion at each digitized time step. An outline of this method is given in the next few paragraphs.

First, the system is excited by a particular ground motion and no control force. Next, the system response $\mathbf{y}_k$ is collected at time step k, which is then modified by a reduction factor c_0, to define $\mathbf{y}_k^0 = c_0 \mathbf{y}_k$ as the *reference uncontrolled system response* at zero control signal, $u_k = 0$, and time step $= k$. Next, the challenge is to find the required control command u_k that achieves the assigned control criteria for the time step k. This can be done by assuming that the control signal that satisfies the control criteria exists somewhere between the upper and lower limits of the control signal ($\mathscr{U}_{\max}$ and $\mathscr{U}_{\min}$). Consequently, the search for this control signal is conducted at each time step. For time step k the control signal u_k is varied alternatively between zero and the upper and lower limits ($\mathscr{U}_{\max}$ and $\mathscr{U}_{\min}$) by increment of Δu as follows:

$$u_{k_j} = u_{k_{j-1}} + j(-1)^j \Delta u, \quad u_0 = 0{\cdot}0, \; j = 1, \ldots, m \tag{2}$$

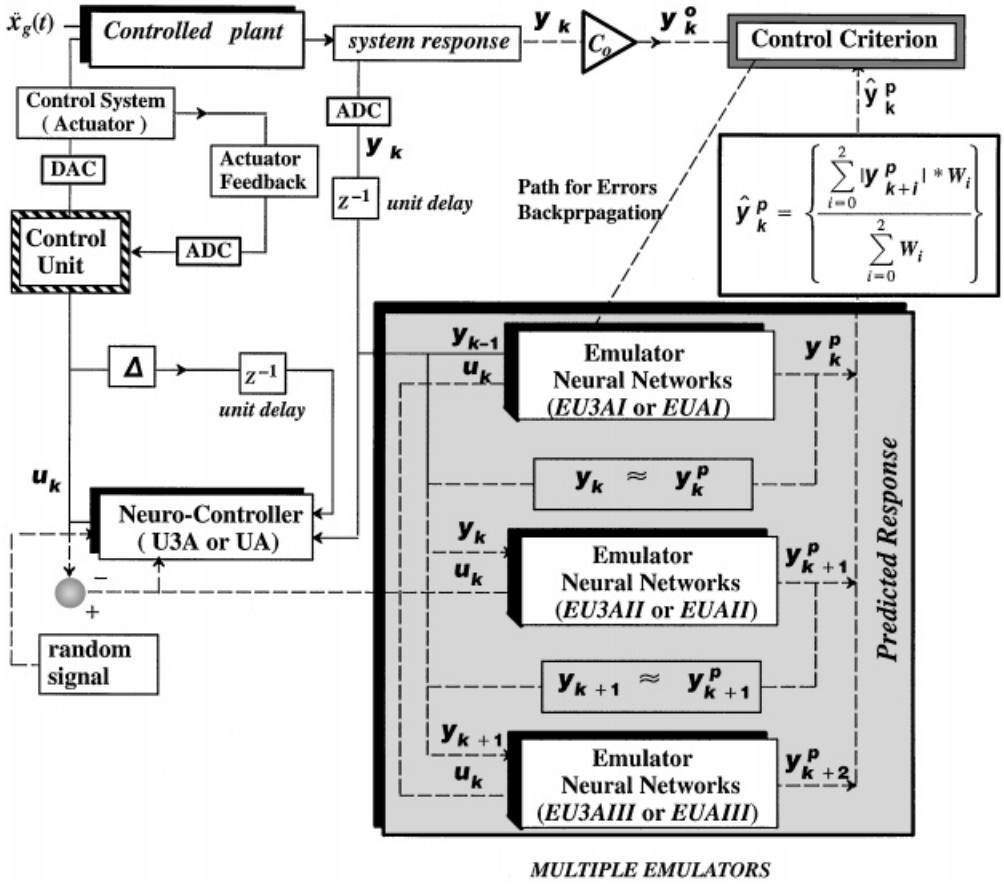

Figure 3. Schematic shows the training method of the neurocontroller with the aid of the multiple emulators neural networks

The value of m reflects the number of control signal trials at each time step and it depends on the required precision:

$$m = (\mathscr{U}_{\max} - \mathscr{U}_{\min})/\Delta u \tag{3}$$

For the time step k the previous time history response $\mathbf{y}_{k-1}$ is available. Then for each $j = 1, \ldots, m$ increment the response $\mathbf{y}_{k-1}$ and its history as well as u_{k_j} defined by equation (2) are fed to the first emulator neural network, EU3AI or EUAI. Consequently, the predicted response at the present time $\mathbf{y}^{\mathrm{p}}_{k_j}$ is collected. Next, the predicted response is assumed to be approximately equal to the system response at time step k, $\mathbf{y}_{k_j} \approx \mathbf{y}^{p}_{k_j}$, and fed to the second emulator network, EU3AII or EUAII, as well as, the current control signal u_{k_j}. The system response $\mathbf{y}^{p}_{k+1_j}$, for the next future time step $k+1$ is predicted and collected. Finally, the predicted responses from the first and the second emulators are assumed to be approximately equal to the actual responses and fed to the third emulator neural network in parallel, EU3AIII or EUAIII, with the same current control

signal u_{k_j}. The third emulator neural network enables us to predict the system response for two time steps ahead $\mathbf{y}^{\mathrm{p}}_{k+2_j}$. In this way, the three emulator neural networks have been used to predict and collect the system responses $\mathbf{y}^{\mathrm{p}}_{k_j}$, $\mathbf{y}^{\mathrm{p}}_{k+1_j}$ and $\mathbf{y}^{\mathrm{p}}_{k+2_j}$ from the previous system response and the control signal u_{k_j}. The predicted responses are used to define a new equivalent system response for signal increment j as follows:

$$\hat{\boldsymbol{y}}^{\mathrm{p}}_{k_j} = \frac{|\boldsymbol{y}^{\mathrm{p}}_{k_j}|\boldsymbol{W}_1 + |\boldsymbol{y}^{\mathrm{p}}_{k+1_j}|\boldsymbol{W}_2 + |\boldsymbol{y}^{\mathrm{p}}_{k+2_j}|\boldsymbol{W}_3}{\sum_{i=1}^{s} W_{1_i} + \sum_{i=1}^{s} W_{2_i} + \sum_{i=1}^{s} W_{3_i}} \tag{4}$$

where $\boldsymbol{W}_i$ are $s \times 1$ vector functions that assign weights to the predicted response according to their importance and their prediction reliabilities.

The estimated equivalent response ($\hat{\boldsymbol{y}}^{\mathrm{p}}_{k_j}$) for control signal u_{k_j} is used with the collected system response at time step k ($\mathbf{y}^0_k$) to check the validation of the control criterion. If the control criterion is met, the control signal u_{k_j} is chosen to be the appropriate control signal for time step k; $u_k = u_{k_j}$. The control criterion can be set by the designer to achieve different control objectives. The following control criterion was used in this study:

$$\hat{\mathbf{y}}^{\mathrm{p}}_{k_j} \leqslant \mathbf{y}^0_{k_j} \quad \text{and} \quad \hat{\mathbf{y}}^{\mathrm{p}}_{k_j} \leqslant \boldsymbol{\varepsilon} \tag{5}$$

The control criterion in equation (5) should be satisfied, otherwise a new iteration for the same time step k is pursued and a new control signal $u_{k_{j+1}}$ is selected for use in the three emulator neural networks. Then the system responses $\mathbf{y}^{\mathrm{p}}_{k_{j+1}}$, $\mathbf{y}^{\mathrm{p}}_{k+1_{j+1}}$ and $\mathbf{y}^{\mathrm{p}}_{k+2_{j+1}}$ are collected and used to estimate $\hat{\mathbf{y}}^{\mathrm{p}}_{k_{j+1}}$ as in equation (4). The equivalent system response, again, is checked for the control criterion given in equation (5). This process is repeated m times for j until the control criterion is satisfied. If the control criterion could not be satisfied through the all choices of u_{k_j}, the control signal that minimizes the equivalent system response is chosen as u_k. This procedure is repeated at each time step k for the duration of the ground motion record chosen to train the neurocontroller. Clearly this method has two nested loops of iterations where the first loop is for the time step $k = 1, \ldots, n$ and the other loop for the control signal increments $j = 1, \ldots, m$. The final training data for the neurocontroller is collected from the control signals that achieved the control criteria and from the associated system response.

Neurocontrollers U3A and UA

Two neurocontrollers have been designed, trained and tested. Neurocontroller U3A uses the absolute accelerations at the three floors as control feedback. Neurocontroller UA uses only the absolute acceleration of the *third floor* as control feedback. In addition, both controllers use the response history of the control command in their input layers. Neurocontroller U3A has 12 input nodes representing the three previous time steps of the control commands (u_{k-1}, u_{k-2} and u_{k-3}) and the three previous time steps of the three floors absolute accelerations ($\ddot{\boldsymbol{x}}_{k-1}, \ddot{\boldsymbol{x}}_{k-2}$ and $\ddot{\boldsymbol{x}}_{k-3}$). The output layer of neurocontroller U3A has one node which represents the control command u_k. Two hidden layers of 7 nodes each were required in training neurocontroller U3A. The number of nodes in each of hidden layer has been determined adaptively using the dynamic node generation method. Neurocontroller UA has 9 input nodes representing the control commands at three previous time steps (u_{k-1}, u_{k-2} and u_{k-3}) and the *third floor* absolute acceleration at the six previous time steps ($\ddot{x}_{3_{k-1}}, \ddot{x}_{3_{k-2}}, \ddot{x}_{3_{k-3}}, \ddot{x}_{3_{k-4}}, \ddot{x}_{3_{k-5}}$ and $\ddot{x}_{3_{k-6}}$). Similarly, the output layer of neurocontroller UA has one output node, which represents the control command

u_k. Two hidden layers of 6 units each have been used in training neurocontroller UA. The architectures of the two neurocontrollers are shown in Figure 1.

The two neurocontrollers, U3A and UA, are symbolically represented by the following equations, using the notation introduced by Ghaboussi and his co-authors:[23]

Neurocontroller U3A:

$$u_k = u_k \mathbf{NN}\,[u_{k-1}, u_{k-2}, u_{k-3}, \ddot{x}_{k-1}, \ddot{x}_{k-2}, \ddot{x}_{k-3}; 12, 7, 7, 1] \tag{6}$$

Neurocontroller UA:

$$u_k = u_k \mathbf{NN}\,[u_{k-1}, u_{k-2}, u_{k-3}, \ddot{x}_{k-1}, \ddot{x}_{k-2}, \ddot{x}_{k-3}, \ddot{x}_{k-4}, \ddot{x}_{k-5}, \ddot{x}_{k-6}; 9, 6, 6, 1] \tag{7}$$

The training data for the neurocontrollers have been obtained using the mentioned control strategy and the emulator neural networks associated with each neurocontroller. Two accelerograms were used for ground excitation in order to develop the training data. The first accelerogram was 25 per cent of the N–S component of the 1940 El Centro, with time compressed by a factor of two, at Imperial Valley Irrigation District, and the second accelerogram was a (0–50) Hz band-limited white noise excitation for 30 s. Neurocontroller U3A has a sampling period of 10 ms, which resulted in 7000 training cases, in which 1000 of these training cases represent the relationship between the neurocontroller response and the feedback inputs when the system is not excited by any ground motion. These additional training cases were included to produce neurocontroller that was less sensitive to the noise sources of software and hardware implementation. Neurocontroller UA has a sampling period of 5 ms, which resulted in 14 000 training cases including 10 s of training period needed for noise sensitivity reduction. It should be mentioned that these neurocontrollers have different sampling periods because the data acquisition and the software implementation of neurocontroller U3A needed more time than neurocontroller UA. Neurocontroller UA has one sensor feedback to process which requires less computation time than neurocontroller U3A. Undoubtedly, in practice, there is a trade-off between the number of sensors used for feedback and the sampling period, and the advantage of using three sensor feedbacks resulted in slower sampling rate, while the using of fewer feedback sensors has led to faster sampling rate.

In the implementation of the control strategy the numerical values of the required parameters have been set such that the control criteria is to reduce the system absolute accelerations. For neurocontroller U3A, $\mathbf{y} = [\ddot{x}_1, \ddot{x}_2, \ddot{x}_3]$, $\mathbf{C}_0 = 0{\cdot}95$, $u_{\text{limits}} = \pm 1{\cdot}0$ V, $\Delta u = 0{\cdot}001$ V, $n = 2000$, $\boldsymbol{W}_1 = [1{\cdot}0\ \ 1{\cdot}5\ \ 2{\cdot}0]^{\mathrm{T}}$, $\boldsymbol{W}_2 = [0{\cdot}85\ \ 1{\cdot}25\ \ 1{\cdot}6]^{\mathrm{T}}$, $\boldsymbol{W}_3 = [0{\cdot}65\ \ 1{\cdot}0\ \ 1{\cdot}25]^{\mathrm{T}}$, $s = 3$ and $\varepsilon = 0{\cdot}15\,g$. Neurocontroller UA has $\mathbf{y} = \ddot{x}_3$, $\mathbf{C}_0 = 0{\cdot}95$, $u_{\text{limits}} = \pm 1{\cdot}0$ V, $\Delta u = 0{\cdot}001$ V, $n = 2000$, $\boldsymbol{W}_1 = [1{\cdot}5]$, $\boldsymbol{W}_2 = [1{\cdot}25]$, $\boldsymbol{W}_3 = [1{\cdot}0]$, $s = 1$ and $\varepsilon = 0{\cdot}15\,g$.

Neurocontroller experimental results, robustness, and stability

The two neurocontrollers have been applied successfully in laboratory experiments. Figure 2 shows a schematic diagram of the experimental set-up. The structure has been extensively tested for both controllers for various types of ground motions. Preliminary testing of the neurocontrollers were established using a numerically simulated model[10] where the effectiveness and robustness with different types of uncertainties and delays were verified. This ensured proper operation and safety of the specimen before the laboratory tests were executed. Experimental results, as shown in Figures 4–7, indicate that the neurocontrollers were successful in mitigating and

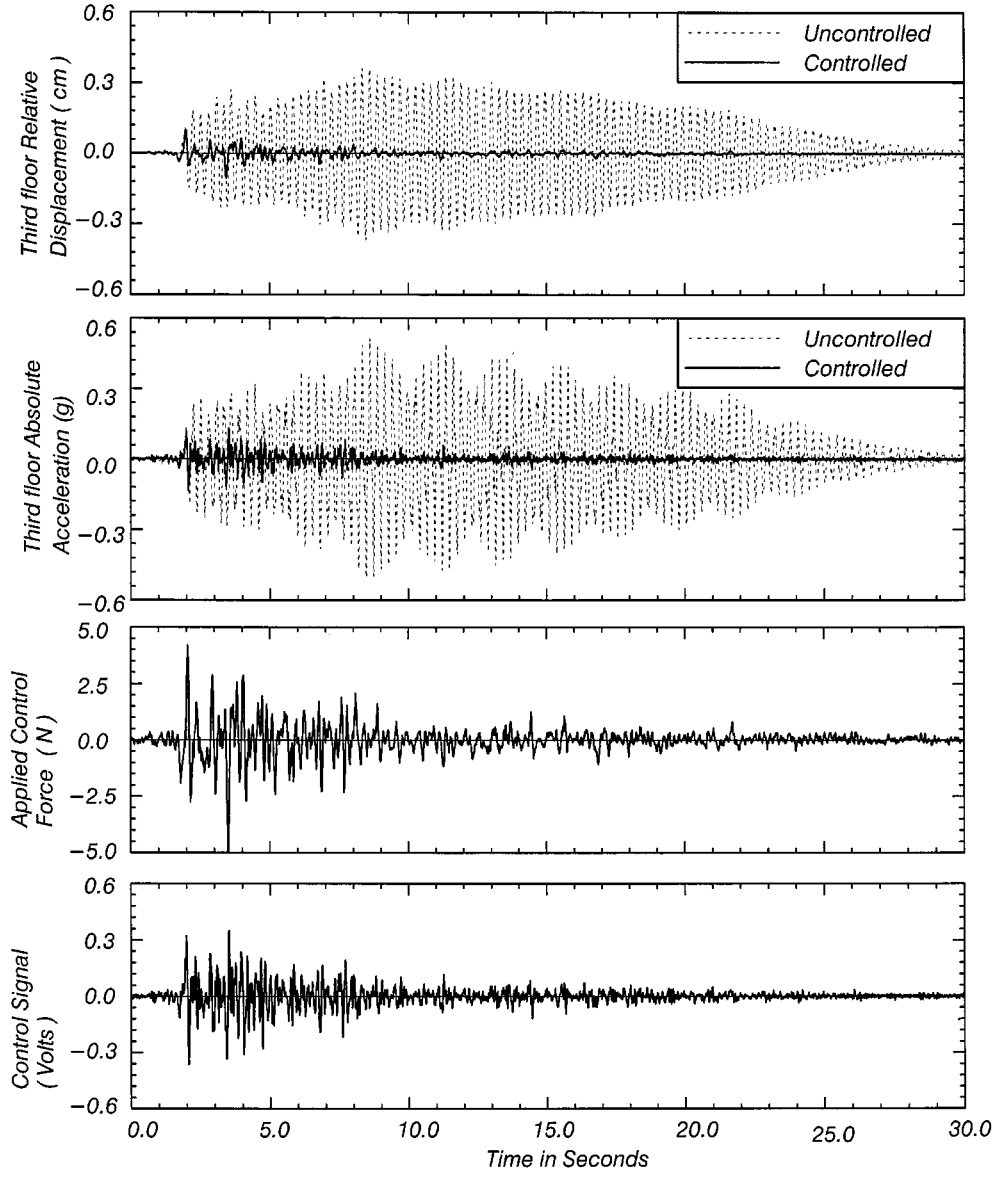

Figure 4. Experimental results of the structural response using neurocontroller U3A. The system was subjected to 50 per cent of Taft earthquake record

reducing the system vibrations effectively. Clearly the response of the structure, relative displacements and absolute accelerations, have been reduced. These figures show the system response when it was subjected to two different earthquake motions; 50 per cent of the 1972 Taft earthquake record, and a near source record of 25 per cent of the Imperial Valley earthquake

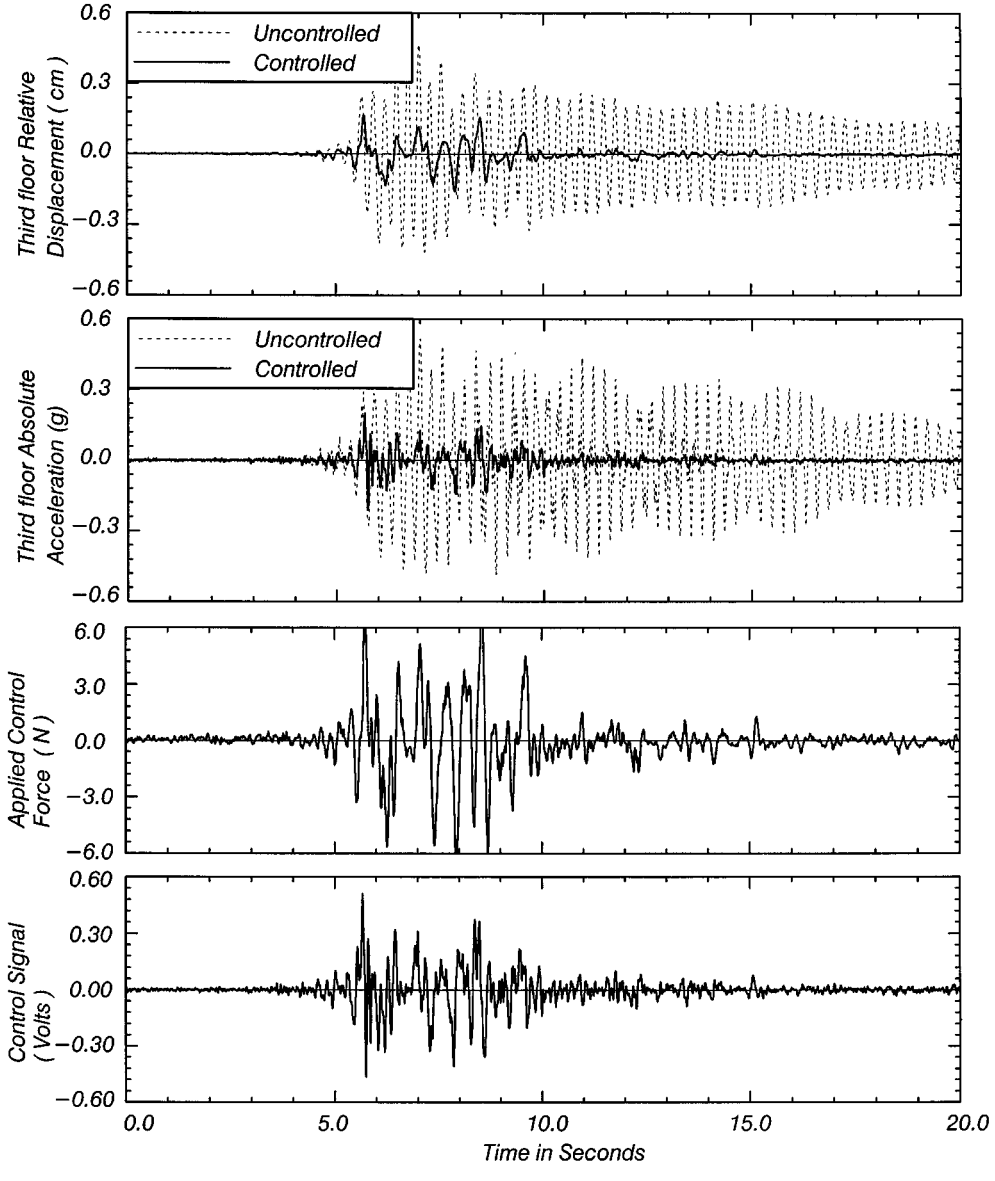

Figure 5. Experimental results of the structural response using neurocontroller U3A. The system was subjected to 25 per cent Imperial Valley earthquake record

record. Figures 8 and 9 show the closed-loop transfer functions for the two controllers compared to the uncontrolled transfer functions. This demonstrates the effect of these neurocontrollers in modelling the system damping characteristics and vibrational modes. However, it should be noted that, neither of the two actual records used for training the neurocontrollers had near source earthquake characteristics. Therefore, the performance of the controllers were not as

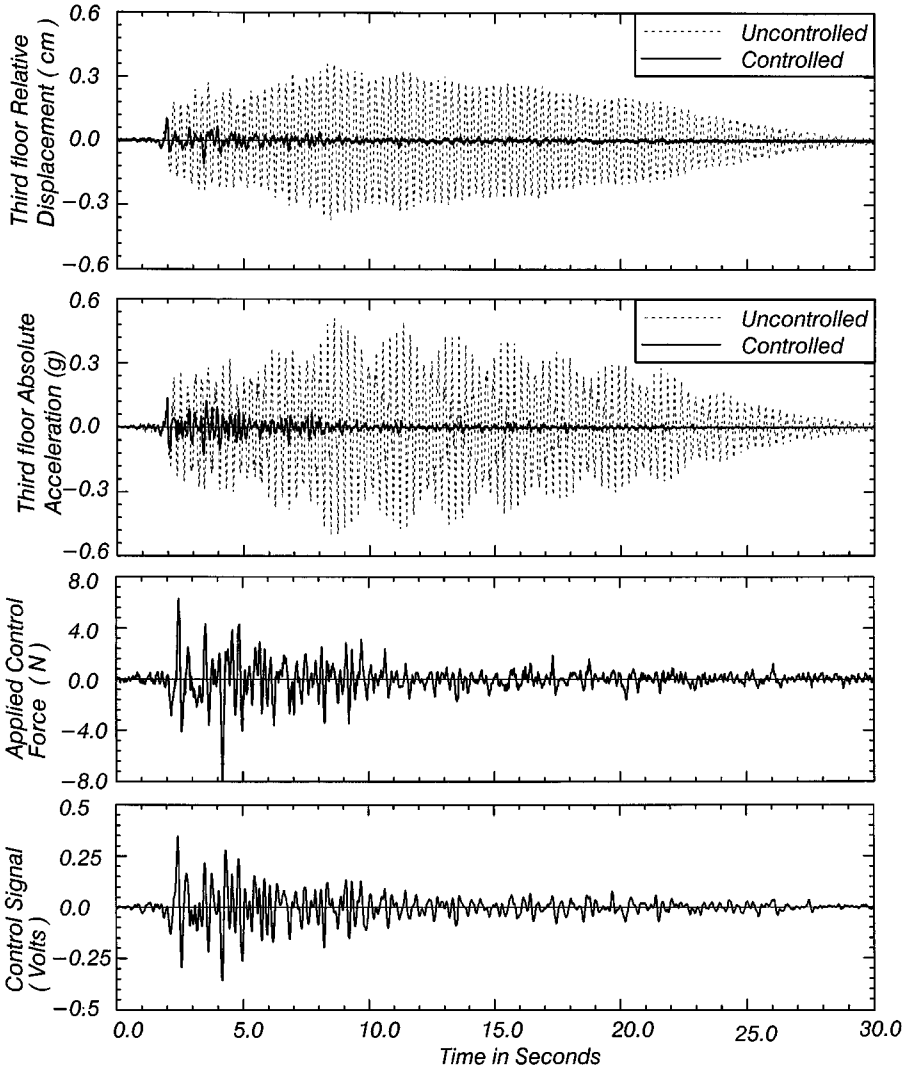

Figure 6. Experimental results of the structural response using neurocontroller UA. The system was subjected to 50 per cent Taft earthquake record

effective when the system was excited by a near source earthquake motion, like the Imperial Valley 1979, N230°E. A numerical comparison between the neurocontrolled response and the uncontrolled response is presented in Table I for El Centro, Taft and Imperial Valley.

The robustness and stability of the neurocontrollers were investigated and verified. Intuitively, a system is said to be stable when it remains at rest unless an external source excites it and returns to rest when the source is removed. The feedback system stability can be established based on the eigenvalues of its closed-loop parameters. However, neurocontrollers involve a combination of

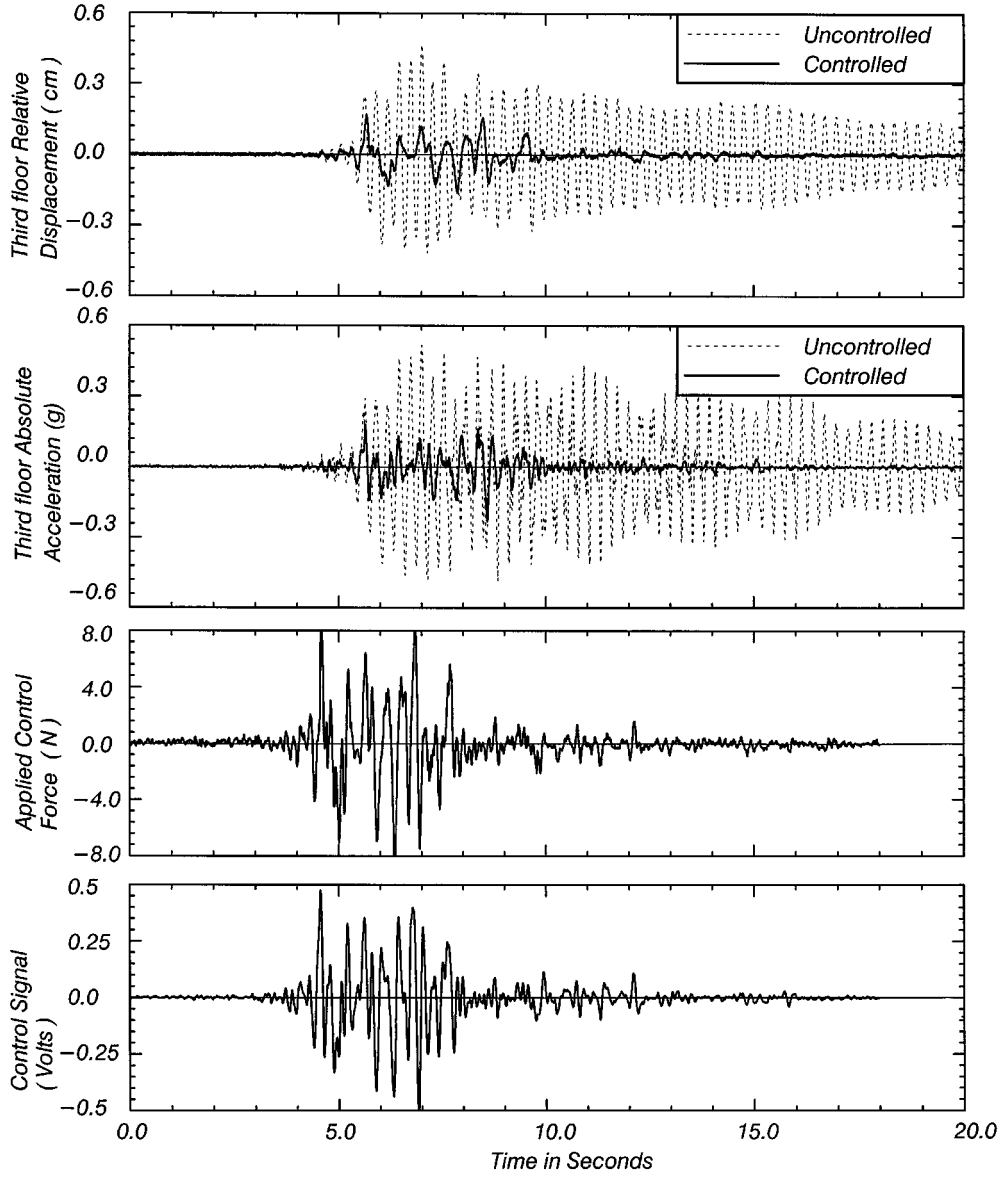

Figure 7. Experimental results of the structural response using neurocontroller UA. The system was subjected to 20 per cent of Imperial Valley earthquake record

highly non-linear functions, which makes it mathematically awkward, if not impossible, to compute the eigenvalues. Therefore, an alternate, graphical method is used to measure the relative stability or how far the system is from instability. First, the loop gain, gain margin, and phase margin are defined. The closed-loop transfer function, $G_{CL}(s)$ in Laplace transform domain, of

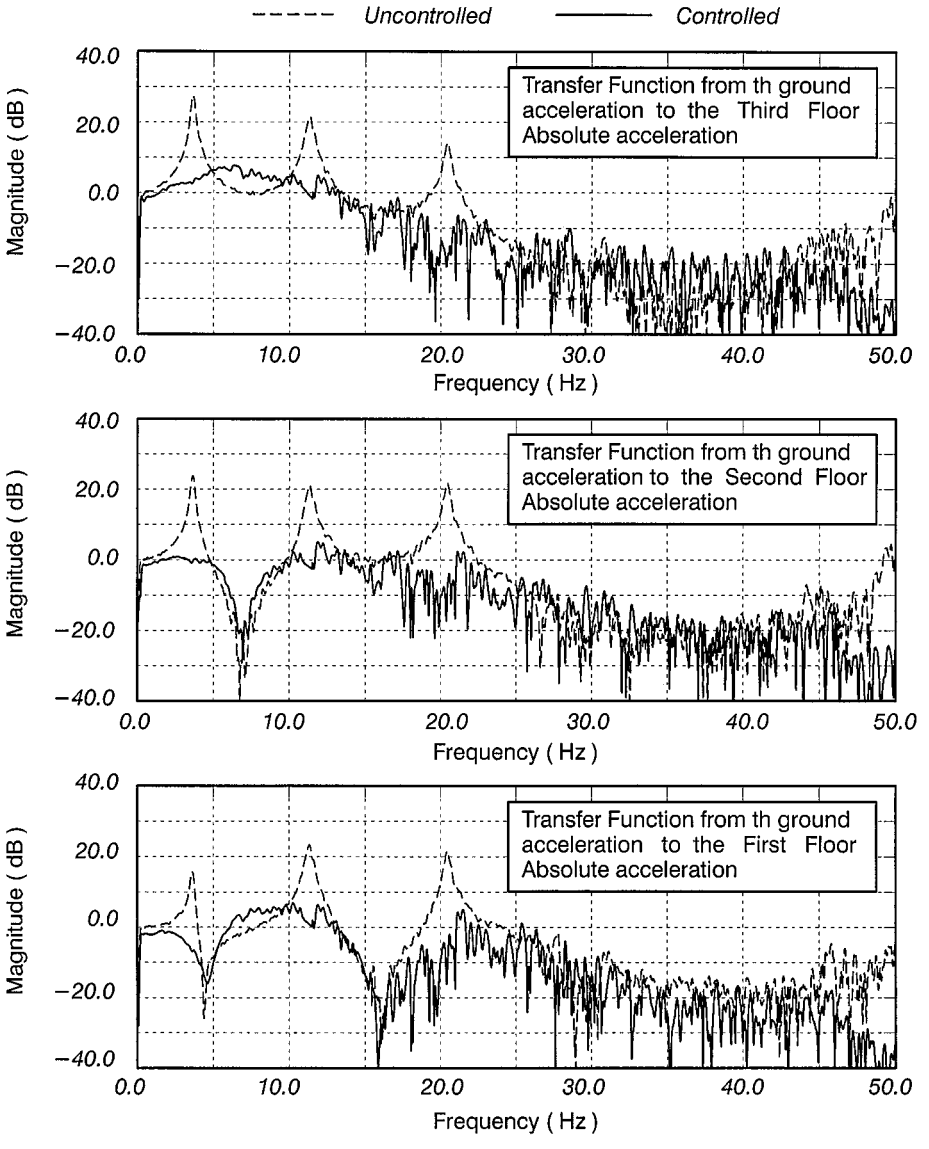

Figure 8. The experimental transfer functions for the uncontrolled and the controlled response, for neurocontroller U3A

a feedback system is described by the system transfer function $G_p(s)$, and the controller transfer function, $G_{NC}(s)$, as follows:

$$\boldsymbol{G}_{CL}(s) = \frac{\boldsymbol{G}_{NC}(s)\boldsymbol{G}_p(s)}{1 + \boldsymbol{G}_{NC}(s)\boldsymbol{G}_p(s)} \tag{8}$$

From equation (8), it is clear that poles of the closed-loop transfer function $\boldsymbol{G}_{CL}(s)$ are closely related to the zeros of the denominator $(1 + \boldsymbol{G}_{NC}(s)\boldsymbol{G}_p(s))$ which is affected by the properties of the

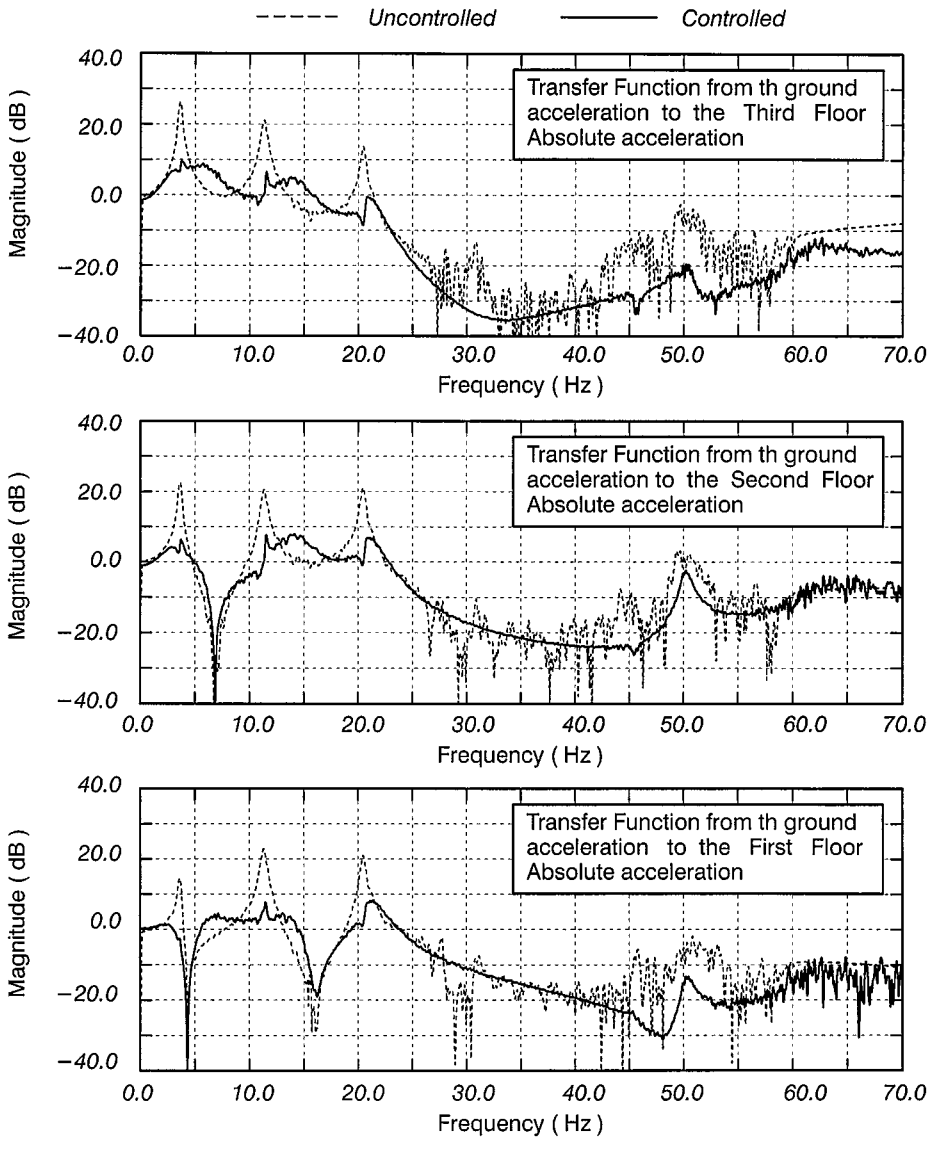

Figure 9. The experimental transfer functions for the uncontrolled and the controlled response, for neurocontroller UA

transfer function $\boldsymbol{G}_{\mathrm{NC}}(s)\boldsymbol{G}_p(s)$. The function $\boldsymbol{G}_{\mathrm{NC}}(s)\boldsymbol{G}_p(s)$ is defined to be the loop-gain transfer function $\boldsymbol{H}_{\mathrm{loop}}(s)$, and can be estimated experimentally by breaking the loop at the control command input as shown in Figure 10. Obviously, the loop gain transfer function $\boldsymbol{H}_{\mathrm{loop}}(s)$ has a strong relation with the closed-loop poles $\boldsymbol{G}_{\mathrm{CL}}(s)$. Hence, a necessary condition for closed-loop stability, is that the loop gain transfer function $\boldsymbol{H}_{\mathrm{loop}}(s)$ is expected to 'roll off' for higher frequencies with magnitudes less than unity.

Table I. Experimental comparison of the peaks and RMS values between the controlled and uncontrolled systems

Controller	$\ddot{x}_1$	$\ddot{x}_2$	$\ddot{x}_3$	x_1	x_2	x_3	x_p	f_c	u_c
Experimental peaks results for 25 per cent of the El Centro earthquake excitation									
Uncontrolled	0·2522	0·3665	0·6035	0·2222	0·5588	0·4597	0·0249	5·1672	—
U3A	0·1035	0·1051	0·1315	0·0706	0·1234	0·0859	0·1715	7·0539	0·5369
UA	0·1011	0·1482	0·1514	0·0757	0·1267	0·0889	0·2570	6·8308	0·4735
Experimental RMS results for 25 per cent of the El Centro earthquake excitation									
Uncontrolled	0·0487	0·0751	0·1080	0·0521	0·1260	0·0975	0·0056	1·1485	—
U3A	0·0107	0·0113	0·0156	0·0104	0·0163	0·0117	0·0262	1·0952	0·0548
UA	0·0099	0·0123	0·0169	0·0109	0·0165	0·0119	0·0392	1·0431	0·0487
Experimental peaks results for 25 per cent of the Imperial Valley earthquake									
Uncontrolled	0·2995	0·3705	0·5168	0·2304	0·5819	0·4661	0·0267	5·2945	—
U3A	0·1567	0·1346	0·2123	0·1537	0·2352	0·1684	0·2896	6·6182	0·5601
UA	0·1529	0·1549	0·2327	0·1549	0·2360	0·1709	0·4341	5·927	0·5388
Experimental RMS results for 25 per cent of the Imperial Valley earthquake									
Uncontrolled	0·0722	0·1009	0·1449	0·0693	0·1664	0·1285	0·0074	1·5239	—
U3A	0·0190	0·0194	0·0261	0·0282	0·0422	0·0272	0·0457	0·9946	0·0583
UA	0·1810	0·0216	0·0302	0·0284	0·0422	0·0274	0·0686	0·8919	0·0488
Experimental peaks results for 50 per cent of the Taft earthquake excitation									
Uncontrolled	0·2618	0·3636	0·5125	0·1986	0·4658	0·3693	0·0241	4·6304	—
U3A	0·1081	0·1148	0·1355	0·0894	0·1420	0·1069	0·2047	5·2638	0·4052
UA	0·0946	0·1102	0·1375	0·0902	0·1453	0·1102	0·3071	4·8952	0·3547
Experimental RMS results for 50 per cent of the Taft earthquake excitation									
Uncontrolled	0·0709	0·1071	0·1547	0·0742	0·1796	0·1389	0·0089	1·6364	—
U3A	0·0138	0·0130	0·0177	0·0107	0·0165	0·0119	0·0221	0·5636	0·0388
UA	0·0105	0·0114	0·0184	0·0112	0·0170	0·0122	0·0330	0·4456	0·0305

The gain and the phase margins are closely related to the closed-loop stability. The gain margin is defined as how much the feedback gain (gain loop) can be increased before instabilities results. Similarly, the phase margin is defined by how much the loop gain $\boldsymbol{H}_{\text{loop}}(s)$ phase shift at unity gain can be changed before the closed-loop system becomes unstable. These two margins can be read directly from the experimental plot of the loop gain transfer function $\boldsymbol{H}_{\text{loop}}(s)$. The closed-loop system is considered to be stable if and only if the gain margin of the loop gain is less than unity (less than 0 in decibles), as shown in equation (8). In practice, values of gain margin between 5 and 12 dB is an indication of a good stability design where values of phase margin should range between 40° and 60°.

Examining the two loop gain transfer functions of the two systems associated with the two neurocontrollers, shown in Figure 10, it is noticed that their magnitudes 'roll off' for frequencies higher than 50 Hz with gain magnitudes of less than -6 dB. These observations indicated that the closed-loop system is robust and stable for the designed range of frequencies. Furthermore, the gain margins and the phase margins have been estimated directly from the gain loop transfer functions using a MATLAB[24] code, where their numerical values showed that the feedback systems are stable and robust, these values are also given in Figure 10.

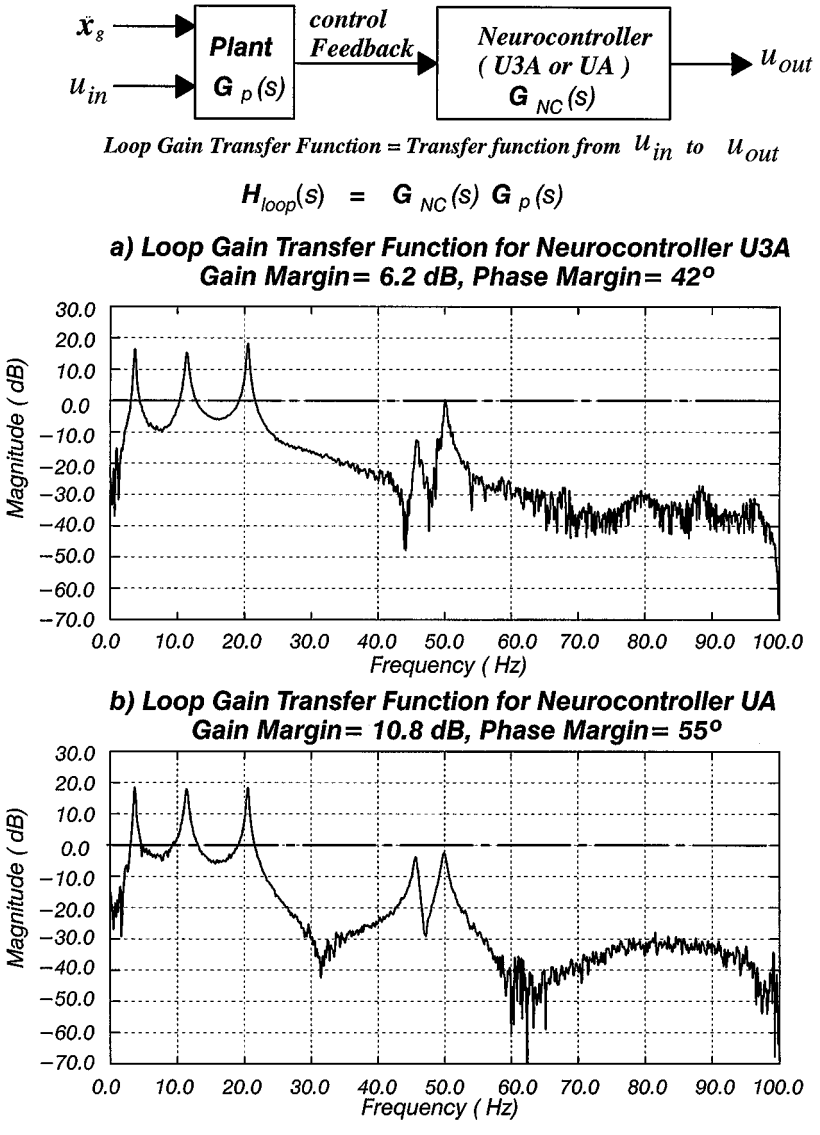

Figure 10. The loop gain transfer function of both neurocontroller (U3A and UA)

Experimental robustness of neurocontroller U3A has been demonstrated in the laboratory set-up. In these experiments different feedback sensors were disconnected intentionally, and the controller performance was monitored and recorded. Four cases, of different combinations of disconnected sensors were tested. Figure 11 shows the controller robustness for these different cases. It was noticed that the neurocontroller maintained its stability for these cases, but its effectiveness was degraded. It can be stated that when the third floor sensor was disconnected a catastrophic effect on the performance of the controller was observed, but yet it remained stable.

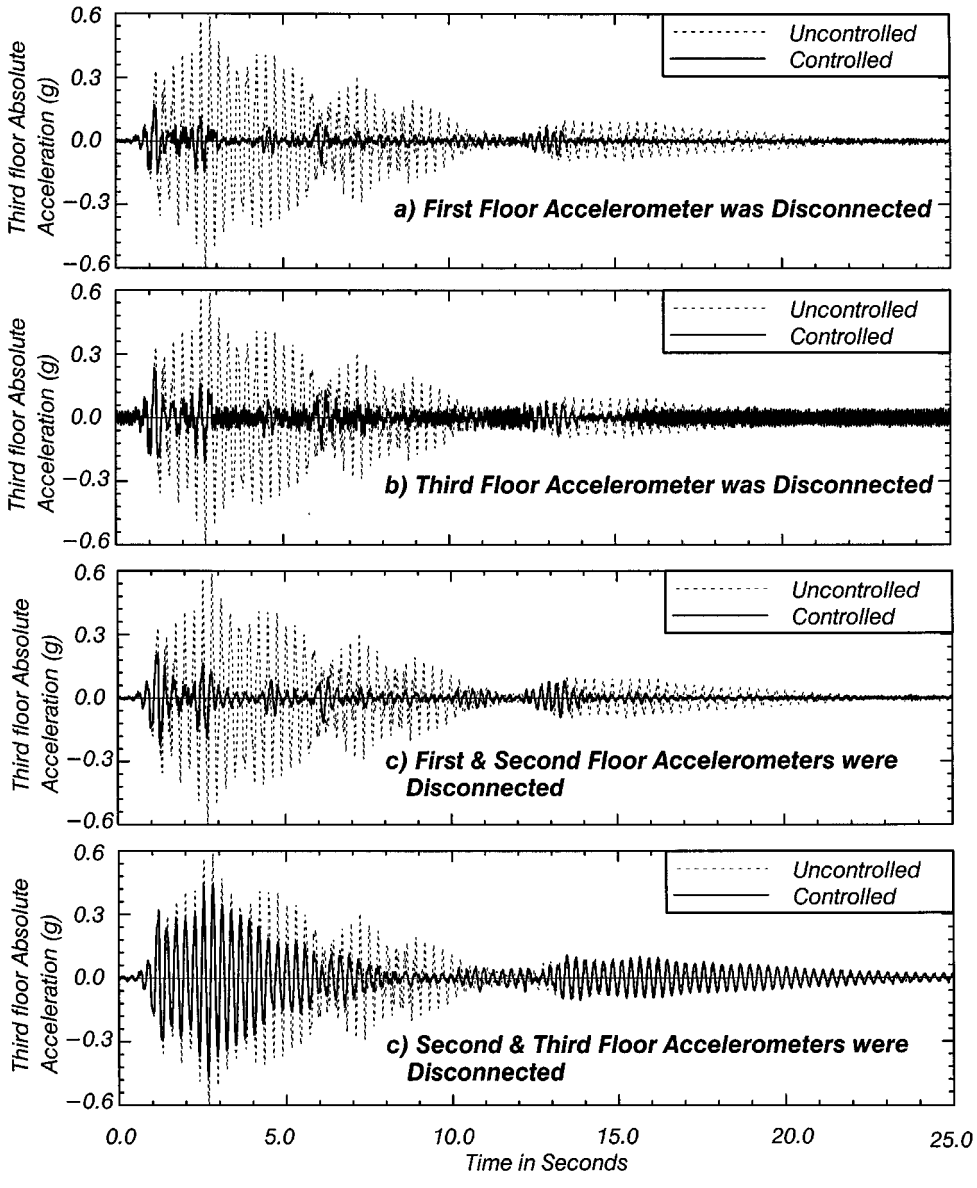

Figure 11. Experimental results of the third floor absolute acceleration when some feedback sensors for neurocontroller U3A are disconnected. The system was subjected to 25 per cent El Centro earthquake record

Moreover, the controller performance was very poor for the fourth severe case, when the second and the third floor sensors were disconnected. These results were expected since the third floor absolute acceleration had feedback information that cannot be compensated with the other feedback sensors. However, when the first floor sensor, for example, was disconnected the degradation of the performance was not severe. This was due to the fact that the first floor sensor

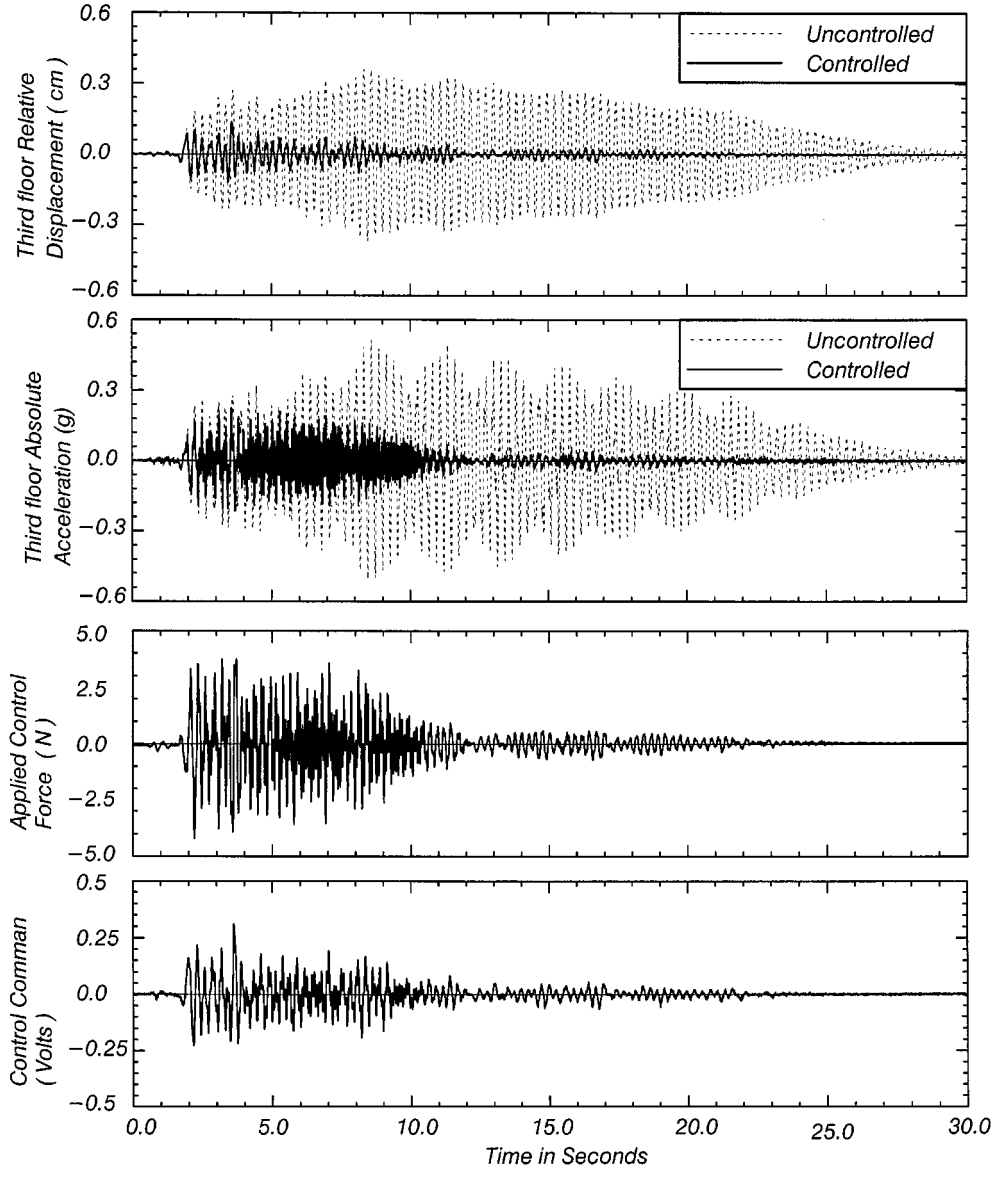

Figure 12. Experimental results of the structural response using the optimal controller. The system was subjected to 50 per cent of Taft earthquake record

information was directly related to the control actuator displacement and the control command was still part of the feedback information. For this reason the choice of the third floor absolute acceleration as feedback for neurocontroller UA was made. In conclusion, these tests and the previous presentation showed that the feedback system is robust and stable for practical implementations.

Comparison between Linear Quadratic Regulator (LQR) and neurocontroller U3A

A linear quadratic regulator, or simply optimal controller, with Kalman[25] state space estimator was developed and tested on the 1/4 scale specimen. The goal of the optimal controller was to compare the conventional controller performance with the neurocontroller performance. The three floor absolute accelerations were used in the state space estimator. They were also used as the feedback in the digital implementation of the optimal controller. The digital optimal controller problem statement was to develop a discrete linear time-invariant state space of the following form:

$$\mathbf{x}_{k+1} = \mathbf{A}_c\mathbf{x}_k + \mathbf{B}_c\mathbf{y}_k \tag{9}$$

$$u_k = \mathbf{C}_c\mathbf{x}_k + \mathbf{D}_c\mathbf{y}_k \tag{10}$$

Optimal control methods are based on a minimization procedure of a specified objective function. The objective function defines a performance index and depends on some constant parameters that are related to the control criteria.[26] The three floor absolute accelerations were used in the objective function minimization, with equal weighting functions. In the optimal controller design it was intended to have the absolute accelerations of the three floors for the feedbacks and a 10 ms sampling period to represent a justified comparison with neurocontroller U3A which uses the same feedbacks and the same sampling period.

The linear quadratic optimal controller was tested experimentally for different ground motions. Figure 12 shows sample results of the performance of the optimal controller when the system was excited by 50 per cent of 1952 Taft earthquake ground motion. Clearly, the optimal controller was able to reduce the system response, however, it is clear that it has some problems in reducing the system accelerations. Figure 13 shows a comparison of the experimental results of the system response for the optimal controller and neurocontroller U3A for two different ground motions; 25 per cent of 1940 El Centro Earthquake record, and 50 per cent of 1952 Taft Earthquake record. The inability of the optimal controller in reducing the system accelerations is seen as weakness of this method. These differences exist for at least three reasons: (1) the neurocontroller has been trained using the emulator neural networks which have been trained from the real experimental set-up behaviour, including the system uncertainties, delays, actuator dynamics, actuator saturation, and control–structure interaction, while the optimal controller has been developed from the identified system[1] which is an approximate model of the real system, (2), the control criteria in the neurocontroller is based on the time average of the future response which creates smoother controller reaction and produces a gradual transition between the signals, thereby, reducing undesirable vibration effects of the controller itself, and (3) the neurocontroller compensated for the 10 ms sampling period while the optimal controller could not compensate for the time delay. However, it is important to note that the optimal controller performance can be improved if the sampling rate is increased, which depends on the speed of the computer and data acquisition system.

CONCLUDING REMARKS

Experimental verification of a neural network based structural control method has been presented and evaluated. Two different types of control strategies were employed in this study. First, two neurocontrollers with different architectures, sensor feedbacks and sampling rates were designed, trained, and tested. The experimental design of the neurocontrollers was achieved with the aid of multiple emulator neural networks (neuro-identifiers) with different prediction

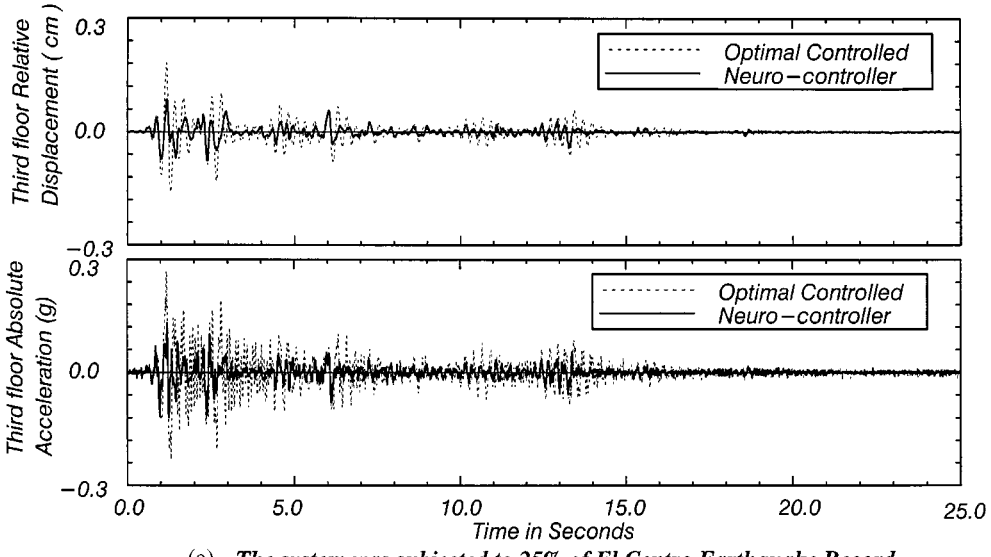

(a) ***The system was subjected to 25% of El Centro Earthquake Record***

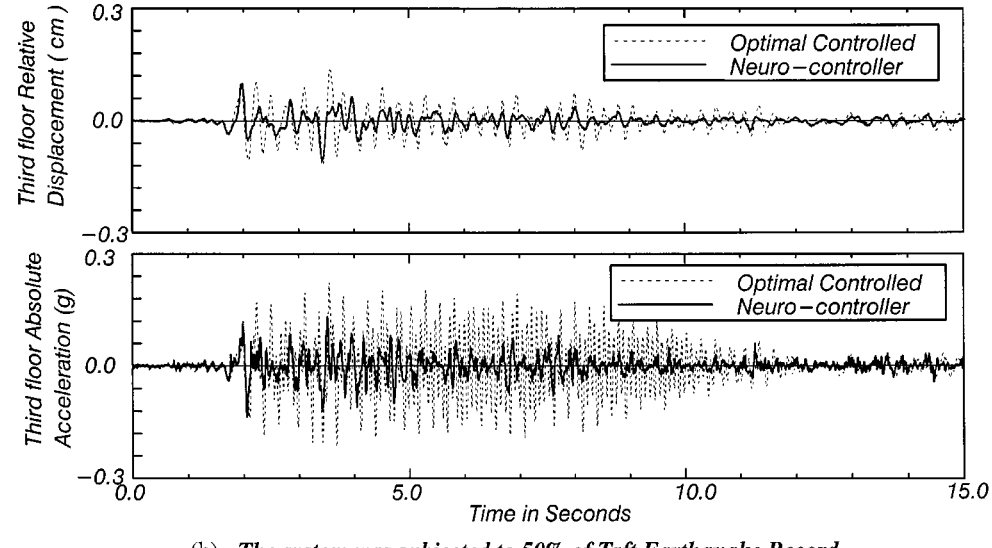

(b) ***The system was subjected to 50% of Taft Earthquake Record***

Figure 13. Experimental comparison between neurocontroller U3A and the optimal controller. The system was subjected to (a) 25 per cent of El Centro earthquake record, (b) 50 per cent of Taft earthquake record

capabilities. The performance of the neurocontrollers showed the potential powerful capabilities in the structural control system. The neurocontrollers were verified for robustness and stability from experimental results. The second type of controller was the linear quadratic Toptimal controller, where it has been developed from the identified model[10] and tested on the experimental specimen. The performances of the neurocontroller and the optimal controller were

compared and studied experimentally, and the relative advantages of the neuro-controllers were illustrated. This study presents the first use of neural networks in active control experiments.

ACKNOWLEDGEMENTS

The research reported in this paper was funded by National Science Foundation Grant CMS-95-003209. This support is gratefully acknowledged.

REFERENCES

1. J. T. P. Yao, 'Concept of structural control', *J. Struct. Engng*, ASCE **98**(6), 1567–1574 (1970).
2. H. H. Leipholz, (ed.) 'Structural control', *Proc. 2nd Int. Symp. on Structural Control 1985*, University of Waterloo, Ontario, Canada, 1987.
3. G. W. Housner, S. F. Masri and A. G. Chassiakos (eds.), *Proc. 1st World Conf. on Structural Control*, 1 WCSC, 3–5 August, Los Angeles, CA, 1994.
4. L. L. Chung, A. M. Reinhorn and T. T. Soong, 'Experiments on active control of seismic structures', *J. Engng Mech. Div* ASCE **114**, 241–256 (1988).
5. J. Rodellar, L. L. Chung, T. T. Soong and A. M. Reinhorn, 'Experimental digital control of structures', *J. Engng. Mech. Div.* ASCE **115**, 1245–1261 (1989).
6. T. T. Soong, A. M. Reinhorn and Y. P. Wang, 'Full scale implementation of active control, design and simulation', *J. Struct. Engng Div.* ASCE **117**(11), 3516–3536 (1991).
7. A. M. Reinhorn, T. T. Soong and M. A. Riley, 'Full scale implementation of active control; installation and performance', *J. Struct. Engng. Div.* ASCE **119**(6), 1935–1960 (1993).
8. S. J. Dyke, B. F. Spencer, P. Quast, D. Kaspari Jr. and M. K. C. Sain, 'Implementation of active mass driver using acceleration feedback control', *Microcomput. Civil Engng.*, **11**, 305–323 (1996).
9. S. J. Dyke, B. F. Spencer, B. Quast and M. K. Sain, 'Acceleration feedback control of MDOF structures', *J. Engng. Mech. Div.* ASCE **122**(9), 907–918 (1996).
10. K. Bani-Hani, J. Ghaboussi and S. P. Schneider, 'Experimental study of identification and control structures using neural network. Part 2: identification', *Earthquake Engng. Struct. Dyn.*, **28**, 995–1018 (1999).
11. K. Nikzad and J. Ghaboussi, 'Application of multi-layered feedforward neural networks in digital vibration control', *Proc. Int. Joint Conf. on Neural Networks*, II-A1004, Seattle, 1991.
12. K. Nikzad, J. Ghaboussi and S. L. Paul, 'A study of actuator dynamics and delay compensation using neuro-controllers', *J. Engng. Mech.* ASCE **122**(10), 966–975 (1996).
13. J. Ghaboussi, 'Some applications of neural networks in structural engineering', *Proc. Structures Congress '94*, ASCE, Atlanta, GA, 1994.
14. A. Joghataie and J. Ghaboussi,'Neural networks and fuzzy logic in structural control', *Proc. 1st World Conf. on Structural Control*, 3–5 August, IASC, Los Angeles, CA, 1994, pp. Wp1-21–wp1-30.
15. J. Ghaboussi and A. Joghatai, 'Active control of structures using neural networks', *J. Engng. Mech. Div.* ASCE **121**(4), 555–567 (1995).
16. J. Ghaboussi and K. Bani-Hani, 'Neural network based nonlinear structural control methods', *Proc. 2nd Int. Workshop on Structural Control*, IASC, Hong Kong, 18–21 December 1996.
17. K. Bani-Hani and J. Ghaboussi, 'Nonlinear structural control using neural networks', *J. Engng. Mech. Div.* ASCE **124**(3), 319–327 (1998).
18. K. Bani-Hani and J. Ghaboussi, 'Neural networks for structural control of a benchmark problem, active tendon system', *J. Earthquake Engng Struct. Dyn. Special Issue of Benchmark Comparison*, in press.
19. K. Bani-Hani, J. Ghaboussi and S. P. Schneider, 'Experimental study of neural networks based-structural control', *Proc. the 6th U.S. National Conf. on Earthquake Engineering*, Seattle, Washington, 1998.
20. K. Bani-Hani, J. Ghaboussi and S. P. Schneider, 'Experimental study of structural control using neural networks', *Proc. 2nd World Conf. on Structural Control*, Kyoto, Japan, 1998.
21. H. M. Chen, K. H. Tsai, G. Z. Qi and J. C. S. Yang, 'Neural network for structural control', *J. Comput. Civil Engng.* ASCE **9**(2), 168–176 (1995).
22. National Instruments Corporation, *LabVIEW*, Austin, TX, 1994.
23. J. Ghaboussi, D. A. Pecknold, M. Zhang and R. M. HajAli, 'Autoprogressive training of neural network constitutive models', *Int. J. Numer. Meth. Engng.*, **42**, 105–126 (1998).
24. The Math Works, Inc., *MATLAB*, Natick, MA, 1994.
25. B. C. Kuo, *Automatic Control System*, Prentice-Hall, Engelwood Cliffs, NJ, 1982.
26. H. Kwakernaak and R. Sivan, *Linear Optimal Control Systems*, Wiley, New York, 1972.

